

Selected strong decay modes of $Y(4260)$ Yubing Dong,^{1,2} Amand Faessler,³ Thomas Gutsche,³ and Valery E. Lyubovitskij^{3,4}¹*Institute of High Energy Physics, Beijing 100049, P. R. China*²*Theoretical Physics Center for Science Facilities (TPCSF), CAS, Beijing 100049, P. R. China*³*Institut für Theoretische Physik, Universität Tübingen, Kepler Center for Astro and Particle Physics, Auf der Morgenstelle 14, D-72076 Tübingen, Germany*⁴*Department of Physics, Tomsk State University, 634050 Tomsk, Russia*

(Received 29 October 2013; published 18 February 2014)

In the present work the $Y(4260)$ resonance is considered as a weakly bound state of a pseudoscalar D and an axial D_1 charm meson. We consider the two-body decay $Y(4260) \rightarrow Z_c(3900)^\pm + \pi^\mp$, where $Z_c(3900)^\pm$ is treated as hadron molecule as well. Moreover we compute the $Y(4260)$ decay modes $J/\psi\pi^+\pi^-$, recently observed by the BESIII Collaboration, and $\psi(2S)\pi^+\pi^-$. In the last process both the contact diagram with $DD_1 \rightarrow \psi(nS)\pi^+\pi^-$ and the resonance diagram with $DD_1 \rightarrow Z_c(3900)^\pm + \pi^\mp \rightarrow \psi(nS)\pi^+\pi^-$ are taken into account.

DOI: 10.1103/PhysRevD.89.034018

PACS numbers: 13.25.Gv, 13.30.Eg, 14.40.Rt, 36.10.Gv

I. INTRODUCTION

The recent observation by three collaborations—BESIII [1], Belle [2] and CLEO-c [3]—of the new resonance $Z_c(3900)^\pm$, and its neutral partner $Z_c(3900)^0$ by CLEO-c [3], stimulated several studies of this state originating in different theoretical structure assumptions. Since the observed state can be charged and carries intrinsic charm, the main proposition rests on an interpretation either as a hadronic molecular or as a tetraquark state [4,5].

$Z_c(3900)^{\pm,0}$ states can also play a role in the decay dynamics of the $Y(4260)$, which is also considered as a resonance outside the usual charmonium spectrum. This resonance was first observed by BABAR [6] and later confirmed by the CLEO-c [7] and Belle [8] Collaborations. In the literature different interpretations of the structure of this state were considered (for an overview, see e.g. Ref. [9]): molecular assignment— $DD_1(2420)$ molecular state [9–11], $J/\psi K\bar{K}$ bound state [12], $\chi_{c\rho}$ [13] or $\chi_{c\omega}$ molecular state [14], charmonium interpretation [15], tetraquark [16,17], mixed charmonium-tetraquark state [18], nonresonant explanation of the $Y(4260)$ state (interference of $\psi(4160)$ and $\psi(4415)$ charmonia states) [19], hybrid $c\bar{c}g$ [20], hybrid mesons (mixing of $c\bar{c}$ and $c\bar{c}g$) [21], and baryonium $\Lambda_c^+\Lambda_c^-$ bound state [22]. Note that in the coupled-channel model proposed in [23], it was noticed that there is no pole associated with the $Y(4260)$ state. In addition, the production and decay of $Y(4260)$ via $e^+e^- \rightarrow Y(4260) \rightarrow J/\psi\pi^+\pi^-$ was also studied in Ref. [24]. The study of this reaction chain can be an important check for the inner structure of the intermediate state $Y(4260)$.

Based on the hadronic molecular scenario, in Ref. [5] we considered the $Z_c(3900)$ and a possible $Z_c'(3950)$. In a phenomenological Lagrangian approach [25–31], we studied the strong decay widths for $Z_c(3900)^\pm \rightarrow \psi(nS) + \pi^\pm$

or $h_c(mP) + \pi^\pm$. To set up the bound state structure of the composite state we use the compositeness condition [32–34] which is the key ingredient of our approach. In Refs. [33,34] and [25–31], it was proved that this condition is an important and successful quantum field theory tool for the study of hadrons and exotic states as bound states of their constituents. Here we adopt a hadronic molecular structure for the $Y(4260)$ state, where the composition is made up of the pseudoscalar $D(1870)$ and the axial $D_1(2400)$ charm mesons.

In this work we analyze the strong two-body decay $Y(4260) \rightarrow Z_c(3900)^\pm + \pi^\mp$ and the three-body decays $Y(4260) \rightarrow J/\psi + \pi^+\pi^-$ and $Y(4260) \rightarrow \psi(2s) + \pi^+\pi^-$ by using the same phenomenological Lagrangian approach developed in Refs. [25–30]. The states $Z_c(3900)$ and $Y(4260)$ are considered as molecular states. In particular, we consider the $Z_c(3900)^\pm$ as hadronic molecules as was previously discussed in Refs. [4]. $Z_c(3900)^\pm$ together with the neutral partner $Z_c(3900)^0$ form the isospin triplet with the spin and parity quantum numbers $J^P = 1^+$,

$$|Z_c^I(3900)\rangle = \frac{1}{2}|\bar{D}^*\tau^I D + \bar{D}\tau^I D^*\rangle, \quad I = +, -, 0. \quad (1)$$

We also consider the $Y(4260)$ state as a isosinglet molecular state,

$$|Y(4260)\rangle = \frac{1}{2}|\bar{D}_1 D + \bar{D} D_1\rangle, \quad (2)$$

with $J^P = 1^-$. Here $D = (D^+, D^0)$, $D^* = (D^{*+}, D^{*0})$, $D_1 = (D_1^+, D_1^0)$ are the doublets of pseudoscalar, vector and axial-vector D mesons; $\tau^{\pm,0}$ are the isospin matrices defined in terms of the triplet of Pauli matrices τ^i as

$$\tau^\pm = \frac{1}{\sqrt{2}}(\tau^1 \mp i\tau^2), \quad \tau^0 = \tau^3. \quad (3)$$

This paper is organized as follows. In Sec. II we briefly review the basic ideas of our approach and show the effective Lagrangians for our calculations. Then, in Sec. III, we proceed to estimate the widths of the strong two-body $Y(4260) \rightarrow Z_c(3900)^\pm + \pi^\mp$ and three-body $Y(4260) \rightarrow \psi(nS) + \pi^+\pi^-$ decays. For the last case we explicitly include the decay amplitude $Y(4260) \rightarrow Z_c^\pm(3900)\pi^\mp \rightarrow$

$\psi(nS)\pi^+\pi^-$. In our analysis we approximately take into account the mass distribution of the $Y(4260)$ state. Finally, we present our numerical results and compare to recent limits set by experiment.

II. BASIC MODEL INGREDIENTS

Our approach to the possible hadron molecules $Z_c(3900)$ and $Y(4260)$ is based on interaction Lagrangians describing the coupling of the respective states to their constituents,

$$\begin{aligned} \mathcal{L}_{Z_c}(x) &= \frac{g_{Z_c}}{2} M_{Z_c} \vec{Z}_c^\mu(x) \int d^4y \Phi_{Z_c}(y^2) (\bar{D}_\mu^*(x+y/2) \vec{\tau} D(x-y/2) + \bar{D}(x-y/2) \vec{\tau} D_\mu^*(x+y/2)), \\ \mathcal{L}_Y(x) &= \frac{g_Y}{2} M_Y Y^\mu(x) \int d^4y \Phi_Y(y^2) (\bar{D}_{1\mu}(x+y/2) D(x-y/2) + \bar{D}(x-y/2) D_{1\mu}(x+y/2)), \end{aligned} \quad (4)$$

where $\vec{Z}_c \vec{\tau} = Z_c^+ \tau^- + Z_c^- \tau^+ + Z_c^0 \tau^3$; y is a relative Jacobi coordinate, and g_{Z_c} and g_Y are dimensionless coupling constants of $Z_c(3900)$ and $Y(4260)$ to the molecular $\bar{D}D^*$ and $\bar{D}D_1$ components, respectively. Here, $\Phi_H(y^2)$ ($H = Y, Z_c$) is the correlation function which describes the distributions of the constituent mesons in the bound states. A basic requirement for the choice of an explicit form of the correlation function $\Phi_H(y^2)$ is that its Fourier transform vanishes sufficiently fast in the ultraviolet region of Euclidean space to render the Feynman diagrams ultraviolet finite. For simplicity we adopt a Gaussian form for the correlation functions. The Fourier transform of this vertex function is given by

$$\tilde{\Phi}_H(p_E^2/\Lambda_H^2) \doteq \exp(-p_E^2/\Lambda_H^2), \quad (5)$$

where p_E is the Euclidean Jacobi momentum. Λ_H stand for the size parameters characterizing the distribution of the two constituent mesons in the $Z_c(3900)$ and $Y(4260)$ systems.

From our previous analyses of strong two-body decays of X, Y, Z meson resonances interpreted as hadron molecules and of the $\Lambda_c(2940)$, $\Sigma_c(2880)$ baryon states we deduced a value of about $\Lambda \sim 1$ GeV [30]. For a very loosely bound system like the $X(3872)$, a size parameter of $\Lambda \sim 0.5$ GeV [29] is more suitable. Once the size parameters and the masses of the bound state systems are chosen,

the respective coupling constants g_H are determined by the compositeness condition [25,30,32–34]. It implies that the renormalization constant of the hadron wave function is set equal to zero with

$$Z_H = 1 - \Sigma'_H(M_H^2) = 0. \quad (6)$$

Here, Σ'_H is the derivative of the transverse part of the mass operator $\Sigma_H^{\mu\nu}$ of the molecular states (see Fig. 1), which is defined as

$$\begin{aligned} \Sigma_H^{\mu\nu}(p) &= g_\perp^{\mu\nu} \Sigma_H(p) + \frac{p^\mu p^\nu}{p^2} \Sigma_H^L(p), \\ g_\perp^{\mu\nu} &= g^{\mu\nu} - \frac{p^\mu p^\nu}{p^2}. \end{aligned} \quad (7)$$

The explicit expression for the coupling constant g_H ($H = Y, Z_c$) resulting from the compositeness condition is

$$\begin{aligned} g_H^{-2} &= \frac{M_H^2}{\Lambda_H^2} \int_0^\infty \frac{d\alpha d\beta}{16\pi^2 \Delta^2} R(\alpha, \beta) \left(1 + \frac{\Lambda_H^2}{2M_2^2 \Delta} \right) \\ &\times \exp \left\{ -\frac{1}{\Lambda_H^2} \left[R(\alpha, \beta) M_H^2 + \alpha M_1^2 + \beta M_2^2 \right] \right\}. \end{aligned} \quad (8)$$

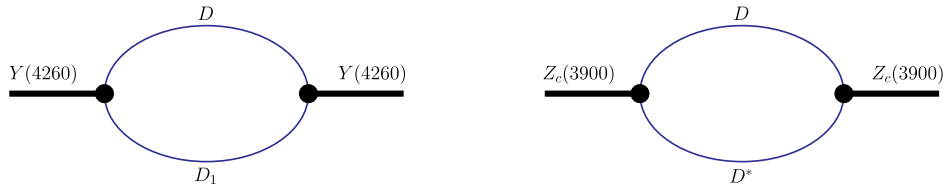


FIG. 1 (color online). Mass operators of $Z_c(3900)$ and $Y(4260)$.

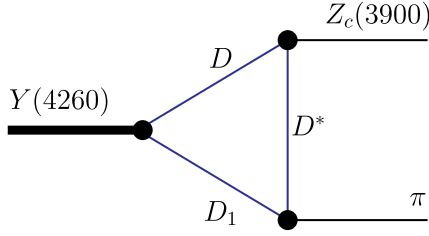


FIG. 2 (color online). Diagram contributing to the $Y(4260) \rightarrow Z_c(3900) + \pi$ decay.

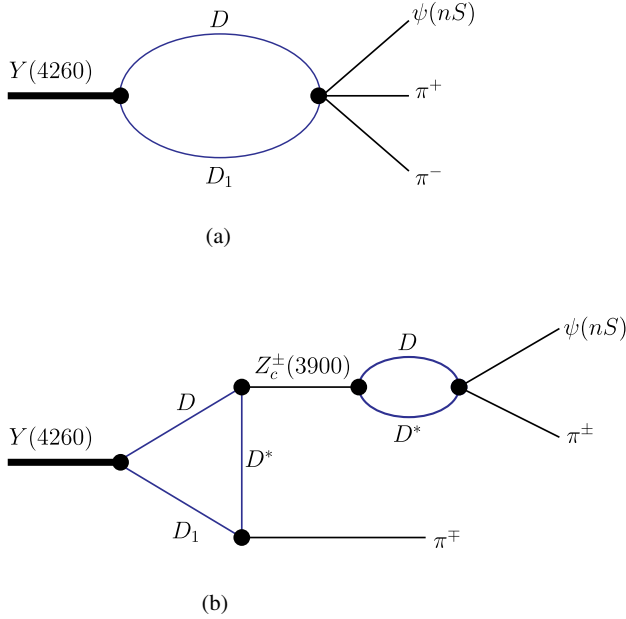


FIG. 3 (color online). Diagrams contributing to the $Y(4260) \rightarrow \psi(nS) + \pi^\pm$ decay: (a) contact diagram, (b) $Z_c(3900)$ resonance diagrams.

In the previous equation we use the notation

$$\Delta = 2 + \alpha + \beta, \quad R(\alpha, \beta) = \frac{(2\omega + \alpha)^2}{\Delta} - (2\omega^2 + \alpha), \quad (9)$$

where $\omega = \frac{M_2}{M_1 + M_2}$, $(M_1, M_2) = (M_D, M_{D^*})$ for $H = Z_c$ and (M_D, M_{D_1}) for $H = Y$, respectively.

In the calculation we use for the $Y(4260)$, the mass $M_Y = 4250 \pm 9$ MeV and width $\Gamma_Y = 108 \pm 12$ MeV [35]. The mass of the $Z_c(3900)$ is expressed in terms of the constituent meson masses and the binding energy ϵ_{Z_c} as

$$M_{Z_c} = M_{D^0} + M_{D^{*0}} - \epsilon_{Z_c}. \quad (10)$$

Note that ϵ_{Z_c} is a variable quantity in our calculations, which we vary from 0.5 to 5 MeV. Once the mass of the composite state Z_c is fixed, the value for the coupling of

TABLE I. Results for the coupling constant g_{Z_c} depending on ϵ_{Z_c} and Λ_{Z_c} .

Λ_{Z_c} in GeV	ϵ_{Z_c} in MeV			
	0.5	1	2.5	5
0.5	2.2	2.3	2.6	3.1
0.75	2.1	2.2	2.5	2.9

$Z_c(3900)$ to DD^* can be extracted from the compositeness condition. Values for this coupling in dependence on the binding energy ϵ_{Z_c} and the cutoff Λ_{Z_c} are shown in Table I. Note that the dependence of g_{Z_c} on the binding energy is in agreement with the scaling law of hadronic molecules found in Ref. [26]: $g_{Z_c} \sim \epsilon_{Z_c}^{1/4}$. Moreover, for the central mass value of the $Y(4260)$, the couplings of $Y(4260)$ to DD_1 are 7.85 for $\Lambda_Y = 0.5$ GeV and 6.25 for $\Lambda_Y = 0.75$ GeV, respectively.

The diagram contributing to the two-body decays $Y(4260) \rightarrow Z_c(3900) + \pi$ is shown in Fig. 2. The diagrams contributing to the $Y(4260) \rightarrow \psi(nS) + \pi^+\pi^-$ transition are drawn in Fig. 3: the contact diagram [Fig. 3(a)] and the resonance diagram [Fig. 3(b)]. For the $Y(4260)$ decays, as presented by the diagrams of Figs. 2 and 3, additional dynamical input is needed. To calculate the two-body decays $Y(4260) \rightarrow Z_c(3900) + \pi$ (Fig. 2) and the resonance diagram corresponding to the transition $Y(4260) \rightarrow Z_c^\pm(3900) + \pi^\mp \rightarrow J/\psi\pi^+\pi^-$ [see Fig. 3(b)], we use the phenomenological Lagrangian for the $D_1 \rightarrow D^*\pi$ coupling with

$$\mathcal{L}_{D_1 D^* \pi} = \frac{g_{D_1}}{2\sqrt{2}} \bar{D}_1^{\mu\nu} \vec{\pi} \vec{\tau} D_{\mu\nu}^* + \text{H.c.}, \quad (11)$$

where $D_1^{\mu\nu}$ and $D_{\mu\nu}^*$ are the stress tensors of D_1 and D^* mesons. The coupling g_{D_1} can be estimated by considering the decay width of $D_1(2420) \rightarrow D^{*+} + \pi^-$ of ~ 20 MeV (see details in Ref. [28]), which is 2/3 of the total $D_1(2420)$ width. Then one gets $g_{D_1} \simeq 0.49$ GeV $^{-1}$.

For the evaluation of the contact diagram in Fig. 3(a), we also need the $DD_1\pi^+\pi^-\psi$ interaction Lagrangian. Such a vertex is derived from a phenomenological Lagrangian recently proposed in Ref. [5] in the analysis of the

TABLE II. Decay widths for $Y(4260) \rightarrow Z_c(3900)^+ + \pi^-$ in MeV.

ϵ_{Z_c} in MeV	$(\Lambda_{Z_c}, \Lambda_Y)$ in GeV			
	(0.5,0.5)	(0.5,0.75)	(0.75,0.5)	(0.75,0.75)
0.5	3.1	2.7	3.1	2.9
1	3.1	2.7	3.2	3.0
2.5	3.3	2.9	3.4	3.2
5	3.4	3.1	3.7	3.6

two-body decays $Z_c^+(Z_c'^+) \rightarrow H + \pi^+$, where $H = \psi(nS)$, $h_c(mP)$ with

$$\mathcal{L}_{\pi^+\pi^-DD_1\psi} = \frac{ig_{DD_1}}{F_\pi^2 M_H} J_{\mu\nu} \bar{D}_{1\mu} D \epsilon_{ijk} \pi_i \partial_\nu \pi_j, \quad g_{DD_1} = 0.6. \quad (12)$$

In the evaluation of Fig. 3(b) the subprocess $Z_c^\pm \rightarrow (DD^*)^\pm \rightarrow \psi(nS) + \pi^\pm$ is treated as worked out in Ref. [5].

III. DECAY MODES AND RESULTS

The two-body decay width for the transition $Y(4260) \rightarrow Z_c(3900) + \pi$ described in Fig. 2 is given by

$$f(m_Y) = \begin{cases} 0, & m_Y < M_{\text{thr}} \\ \frac{1}{4A_0} \cdot \frac{\Gamma_Y^2}{(m_Y - M_Y)^2 + \frac{1}{4}\Gamma_Y^2} \cdot \frac{m_Y - M_{\text{thr}}}{M_Y - \Gamma_Y - M_{\text{thr}}}, & M_{\text{thr}} < m_Y < M_Y - \Gamma_Y \\ \frac{1}{4A_0} \cdot \frac{\Gamma_Y^2}{(m_Y - M_Y)^2 + \frac{1}{4}\Gamma_Y^2}, & M_Y - \Gamma_Y < m_Y < M_Y + \Gamma_Y \\ \frac{1}{4A_0} \cdot \frac{\Gamma_Y^2}{(m_Y - M_Y)^2 + \frac{1}{4}\Gamma_Y^2} \cdot \frac{M_Y + 3\Gamma_Y - m_Y}{2\Gamma_Y}, & M_Y + \Gamma_Y < m_Y < M_Y + 3\Gamma_Y \\ 0, & M_Y + 3\Gamma_Y < m_Y. \end{cases} \quad (15)$$

The lowest strong decay threshold is denoted by $M_{\text{thr}} = M_{J/\psi} + 2M_\pi \approx 3.376$ GeV, and A_0 is a normalization constant such that

$$\int_0^\infty dm_Y f(m_Y) = 1. \quad (16)$$

In Eq. (13) we average the available phase space over the mass distribution of the $Y(4260)$, while the matrix element is evaluated at the central mass value of 4250 MeV. This procedure will capture the major features of the mass distribution of the $Y(4260)$.

The three-body decay width related to the process of Fig. 3 is evaluated as

$$\Gamma_3 = \int_{\psi(nS)+2M_\pi}^{M_Y+3\Gamma_Y} dm_Y \frac{f(m_Y)}{768\pi^3 m_Y^3} \times \int_{(m_2+m_3)^2}^{(m_Y-m_1)^2} ds_2 \int_{s_1^-}^{s_1^+} ds_1 \sum_{\text{pol}} |M_{\text{inv},3}(M_Y)|^2, \quad (17)$$

where $p_{1,2,3}$ and $m_{1,2,3}$ are the momenta and masses of the three outgoing particles, $s_1 = (p_1 + p_2)^2$ and $s_2 = (p_2 + p_3)^2$ are the Mandelstam variables,

$$s_1^\pm = m_1^2 + m_2^2 - \frac{1}{2s_2} ((s_2 - m_Y^2 + m_1^2)(s_2 + m_2^2 - m_3^2) \mp \lambda^{1/2}(s_2, m_Y^2, m_1^2) \lambda^{1/2}(s_2, m_2^2, m_3^2)). \quad (18)$$

$$\Gamma_2 = \int_{M_{Z_c+M_\pi}^{M_Y+3\Gamma_Y}} dm_Y f(m_Y) \frac{|\mathbf{p}(m_Y)|}{24\pi m_Y^2} \sum_{\text{pol}} |M_{\text{inv},2}(M_Y)|^2, \quad (13)$$

where $|\mathbf{p}(m_Y)| = \lambda^{1/2}(m_Y^2, M_{Z_c}^2, M_\pi^2)/(2m_Y)$ is the magnitude of the three-momentum of outgoing particles in the rest frame of the $Y(4260)$ state,

$$\lambda(x, y, z) = x^2 + y^2 + z^2 - 2xy - 2yz - 2xz \quad (14)$$

is the Källén function and $\mathcal{M}_{\text{inv},2}$ is the corresponding invariant matrix element. We consider the finite width of the $Y(4260)$ by setting up a mass distribution $f(m_Y)$ in the form [37,38]

Again, the invariant matrix element of the three-body decay is simply denoted by $\mathcal{M}_{\text{inv},3}(M_Y)$, which is estimated at the central $Y(4260)$ mass $M_Y = 4250$ MeV. The calculation of phase space includes the mass distribution of the $Y(4260)$. The evaluation of the invariant matrix elements in both the two- and three-body decay is standard and not explicitly written out. The calculational technique is, for example, discussed in detail in Ref. [5].

The diagram contributing to the two-body decay $Y(4260) \rightarrow Z_c(3900) + \pi$ is shown in Fig. 2. Numerical results for $\Gamma(Y(4260) \rightarrow Z_c(3900)^+ + \pi^-)$, which are of the order of a few MeV, are given both in Table II and Fig. 4. In our calculations we use two different values for the cutoff parameters Λ_Y and Λ_{Z_c} —0.5 and 0.75 GeV. The dependence of the decay width on the size parameter is only moderate. A larger binding energy ϵ_{Z_c} leads to an increase in phase space and hence in the decay width.

In Tables III and IV we present our numerical results for the widths of both decay modes involving J/ψ and $\psi(2S)$ (in brackets). Results are given for different values of the Z_c binding energy and of the respective size parameters Λ_Y and Λ_{Z_c} . In the calculation of the Z_c resonance contribution, the propagator of Z_c state is described by a Breit-Wigner form, where we have used a constant width Γ_{Z_c} in the imaginary part, i.e. we have used

$$D_{Z_c}(q^2) = \frac{1}{M_{Z_c}^2 - q^2 - iM_{Z_c}\Gamma_{Z_c}}. \quad (19)$$

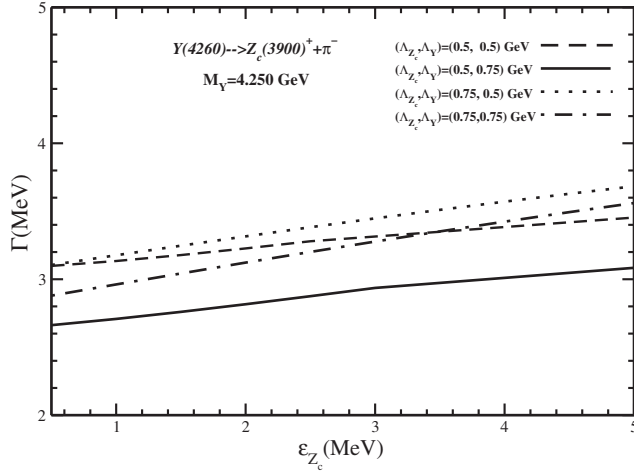


FIG. 4. Decay width $Y(4260) \rightarrow Z_c(3900)^+ + \pi^-$ as function of binding energy $\epsilon_{Z_c} = 0.5 - 5$ MeV and for different cutoff parameters $\Lambda_Y = 0.5, 0.75$ GeV.

We consider two results for Γ_{Z_c} including error bars: $46 \pm 10 \pm 20$ MeV—according to BESIII [1] (see Table III)—and $63 \pm 24 \pm 26$ MeV—the result of the Belle Collaboration [2] (see Table IV). The results for the sole contribution of the contact diagram in Fig. 3(a) are shown in Table V.

For completeness we also plot our results for the three-body decays in Figs. 5–7. In particular, in Fig. 5 we plot the ratio R of resonance diagram [Fig. 3(b)] to total contribution (Fig. 3) to the decay width $Y(4260) \rightarrow J/\psi + \pi^+ \pi^-$ as a function of the binding energy $\epsilon_{Z_c} = 0.5 - 5$ MeV and for different cutoff parameters $\Lambda_Y = 0.5, 0.75$ GeV. The two horizontal lines at $R = 0.201$ and $R = 0.378$ define the lower and upper limit set by data of the Belle Collaboration [2],

$$R = \frac{\text{Br}(Y(4260) \rightarrow Z_c^\pm \pi^\mp) \text{Br}(Z_c^\pm \rightarrow J/\psi \pi^\pm)}{\text{Br}(Y(4260) \rightarrow J/\psi \pi^+ \pi^-)} = (29.0 \pm 8.9)\%. \quad (20)$$

TABLE III. $Y(4260) \rightarrow J/\psi(\psi(2S)) + \pi^+ \pi^-$ decay widths in MeV. Predictions for the mode with $\psi(2S)$ are given in brackets. For total width of $Z_c(3900)$, we use BESIII data $\Gamma_{Z_c} = 46 \pm 10 \pm 20$ MeV [1].

ϵ_{Z_c} in MeV	$(\Lambda_{Z_c}, \Lambda_Y)$ in GeV			
	(0.5,0.5)	(0.5,0.75)	(0.75,0.5)	(0.75,0.75)
0.5	$0.3^{+0.01}_{-0.01}$	$0.8^{+0.01}_{-0.01}$	$0.4^{+0.07}_{-0.02}$	$0.8^{+0.03}_{-0.01}$
	$(0.2^{+0.04}_{-0.01})$	$(0.4^{+0.05}_{-0.02})$	$(0.2^{+0.09}_{-0.03})$	$(0.5^{+0.10}_{-0.04})$
1	$0.3^{+0.02}_{-0.01}$	$0.8^{+0.01}_{-0.01}$	$0.4^{+0.09}_{-0.02}$	$0.8^{+0.06}_{-0.01}$
	$(0.2^{+0.04}_{-0.02})$	$(0.4^{+0.05}_{-0.02})$	$(0.2^{+0.09}_{-0.04})$	$(0.5^{+0.10}_{-0.04})$
2.5	$0.4^{+0.06}_{-0.01}$	$0.8^{+0.04}_{-0.01}$	$0.4^{+0.2}_{-0.04}$	$0.8^{+0.1}_{-0.03}$
	$(0.2^{+0.07}_{-0.02})$	$(0.4^{+0.07}_{-0.03})$	$(0.3^{+0.1}_{-0.05})$	$(0.5^{+0.2}_{-0.06})$
5	$0.4^{+0.2}_{-0.06}$	$0.9^{+0.2}_{-0.04}$	$0.5^{+0.4}_{-0.1}$	$0.9^{+0.4}_{-0.08}$
	$(0.3^{+0.1}_{-0.05})$	$(0.5^{+0.2}_{-0.05})$	$(0.3^{+0.3}_{-0.08})$	$(0.6^{+0.2}_{-0.08})$

TABLE IV. $Y(4260) \rightarrow J/\psi(\psi(2S)) + \pi^+ \pi^-$ decay widths in MeV. Predictions for the mode with $\psi(2S)$ are given in brackets. For total width of $Z_c(3900)$, we use Belle data $(63 \pm 24 \pm 26$ MeV) [2].

ϵ_{Z_c} in MeV	$(\Lambda_{Z_c}, \Lambda_Y)$ in GeV			
	(0.5,0.5)	(0.5,0.75)	(0.75,0.5)	(0.75,0.75)
0.5	$0.3^{+0.01}_{-0.01}$	$0.8^{+0.01}_{-0.01}$	$0.3^{+0.06}_{-0.01}$	$0.8^{+0.02}_{-0.01}$
	$(0.3^{+0.04}_{-0.01})$	$(0.4^{+0.05}_{-0.01})$	$(0.2^{+0.09}_{-0.02})$	$(0.4^{+0.1}_{-0.03})$
1	$0.3^{+0.02}_{-0.01}$	$0.8^{+0.01}_{-0.01}$	$0.4^{+0.08}_{-0.01}$	$0.8^{+0.04}_{-0.01}$
	$(0.3^{+0.04}_{-0.01})$	$(0.4^{+0.05}_{-0.02})$	$(0.2^{+0.1}_{-0.03})$	$(0.4^{+0.1}_{-0.03})$
2.5	$0.3^{+0.05}_{-0.01}$	$0.8^{+0.02}_{-0.01}$	$0.4^{+0.2}_{-0.02}$	$0.8^{+0.1}_{-0.01}$
	$(0.2^{+0.06}_{-0.02})$	$(0.4^{+0.07}_{-0.02})$	$(0.2^{+0.1}_{-0.03})$	$(0.2^{+0.2}_{-0.04})$
5	$0.4^{+0.2}_{-0.03}$	$0.8^{+0.2}_{-0.02}$	$0.5^{+0.4}_{-0.06}$	$0.9^{+0.3}_{-0.04}$
	$(0.2^{+0.1}_{-0.03})$	$(0.5^{+0.2}_{-0.04})$	$(0.3^{+0.2}_{-0.05})$	$(0.5^{+0.2}_{-0.06})$

TABLE V. Contribution of the contact diagram in Fig. 3(a) to $\Gamma(Y(4260) \rightarrow J/\psi(\psi(2S)) + \pi^+ \pi^-)$ in MeV.

Mode	$\Lambda_Y = 0.5$ GeV	$\Lambda_Y = 0.75$ GeV
$Y(4260) \rightarrow J/\psi + \pi^+ \pi^-$	0.26	0.64
$Y(4260) \rightarrow \psi(2S) + \pi^+ \pi^-$	0.12	0.30

As is evident from Fig. 5, the ratio R is rather sensitive to explicit values of the binding energy ϵ_{Z_c} and the choice of size parameters. The present range of values set by Belle can be reproduced in the calculation for restricted values of the varied quantities. In Figs. 6 and 7 we plot the total contributions to the decay rates of $Y(4260) \rightarrow J/\psi \pi^+ \pi^-$

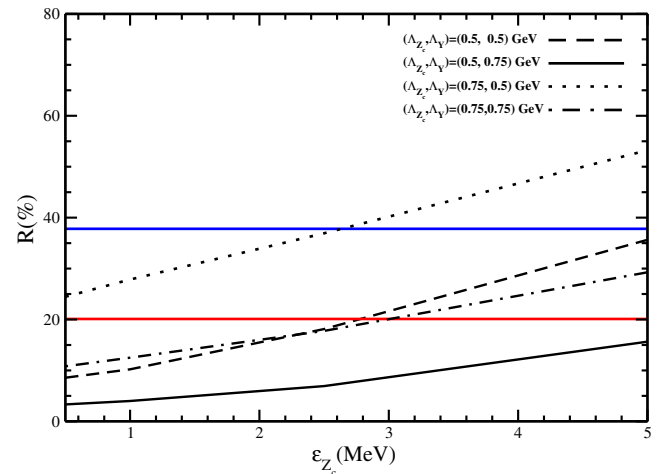


FIG. 5 (color online). Ratio R of the resonance diagram contribution in Fig. 3(b) to the total one (Fig. 3) for the decay width $Y(4260) \rightarrow J/\psi + \pi^+ \pi^-$ as function of the binding energy $\epsilon_{Z_c} = 0.5 - 5$ MeV and for different cutoff parameters $\Lambda_Y = 0.5, 0.75$ GeV. The two horizontal lines at $R = 0.201$ and $R = 0.378$ define the lower and upper limit of data from the Belle Collaboration [2].

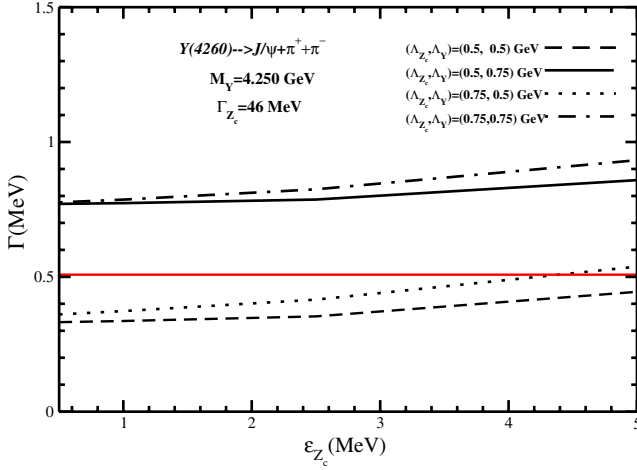


FIG. 6 (color online). Total contribution to the decay width $Y(4260) \rightarrow J/\psi + \pi^+ \pi^-$ as function of the binding energy $\varepsilon_{Z_c} = 0.5 - 5$ MeV and for different values of the cutoff parameters Λ_{Z_c} and $\Lambda_Y = 0.5, 0.75$ GeV. The horizontal line $\Gamma(Y(4260) \rightarrow J/\psi + \pi^+ \pi^-) = 0.508$ GeV corresponds to the lower limit deduced from data in Ref. [36].

and $Y(4260) \rightarrow \psi(2S)\pi^+\pi^-$. In Fig. 6 we indicate the horizontal line $\Gamma(Y(4260) \rightarrow J/\psi\pi^+\pi^-) = 0.508$ MeV corresponding to the lower limit for this decay rate extracted from data of Ref. [36]. From this constraint and from data for the ratio R we estimate that the lower limit of $\Gamma(Y(4260) \rightarrow Z_c^\pm \pi^\mp \rightarrow J/\psi\pi^+\pi^-)$ is larger than 100 keV. Using the last constraint and the results for the ratio R , we conclude that for a favored value of $\Lambda_Y = 0.75$ GeV we deduce a lower limit of $\Gamma(Y(4260) \rightarrow J/\psi\pi^+\pi^-) > 0.8$ MeV. Our results for the favored value of $\Lambda_Y = 0.75$ GeV and including the variation of the cutoff parameter Λ_{Z_c} and of the binding energy ε_{Z_c} can be summarized as

$$\begin{aligned} \Gamma(Y(4260) \rightarrow Z_c^\pm(3900) + \pi^\mp) &= 3.15 \pm 0.45 \text{ MeV}, \\ \Gamma(Y(4260) \rightarrow J/\psi + \pi^+ \pi^-) &= 1 \pm 0.20 \text{ MeV}, \\ \Gamma(Y(4260) \rightarrow \psi(2S) + \pi^+ \pi^-) &= 0.55 \pm 0.15 \text{ MeV}. \end{aligned} \quad (21)$$

In summary, using a phenomenological Lagrangian approach, we give predictions for the two- and three-body decay rates $Y(4260) \rightarrow Z_c^\pm(3900) + \pi^\mp$ and $Y(4260) \rightarrow \psi(nS) + \pi^+ \pi^-$ for $n = 1, 2$. Our results for the two-body decays are in the order of several MeV. For the $Y(4260)$ three-body decay with a charged pion pair, we estimated both contact and $Z_c(3900)$ -resonance contributions, and the decay rate varies from several hundred keV to a few MeV. Both the background and $Z_c(3900)$ contributions are explicitly shown. We expect that the quantitative

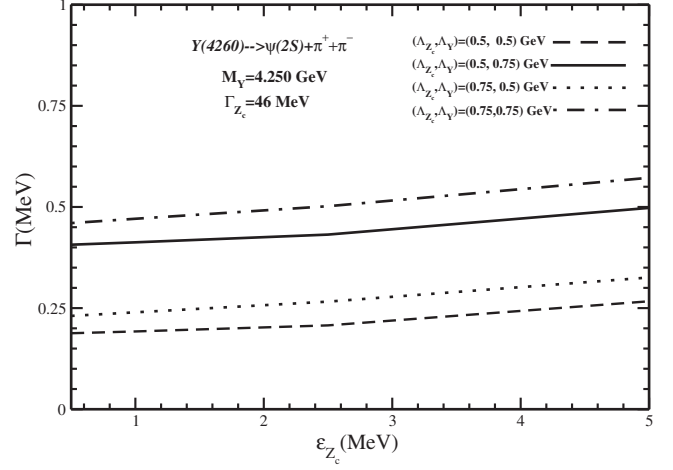


FIG. 7. Total contribution to the decay width $Y(4260) \rightarrow \psi(2S) + \pi^+ \pi^-$ as function of the binding energy $\varepsilon_{Z_c} = 0.5 - 5$ MeV and for different values of the cutoff parameters Λ_{Z_c} and $\Lambda_Y = 0.5, 0.75$ GeV.

predictions given here can serve as a further test for the molecular interpretation of the $Y(4260)$ and can be measured in forthcoming experiments.

In further work we plan to estimate other strong and also radiative decay modes of the $Y(4260)$ state. In particular, the following decay modes of the $Y(4260)$ state can be analyzed: strong decay modes with two heavy charm mesons DD , DD^* or D^*D^* in the final state, the strong decay modes with a h_c state, and radiative decays $Y(4260) \rightarrow Z_c^0(X(3872)) + \gamma$. Special attention will be paid to an analysis of other possible hidden charm resonances [in addition to $Z_c(3900)$] with spin-parities $0^\pm, 1^\pm$ and with a mass in the interval 3900–4100 MeV, all contributing to the total width of the $Y(4260)$ state.

ACKNOWLEDGMENTS

We thank Alex Bondar, Qiang Zhao, Dian Yong Chen and Changzheng Yuan for useful discussions. This work is supported by the DFG under Contract No. LY 114/2-1, the National Sciences Foundations of China Grants No. 10975146 and No. 11035006, and by the DFG and the NSFC through funds provided to the sino-German CRC 110 ‘‘Symmetries and the Emergence of Structure in QCD.’’ The work is done partially under the Project No. 2.3684.2011 of Tomsk State University. V. E. L. would like to thank Tomsk Polytechnic University, Russia, for warm hospitality. Y. B. D. thanks the Institute of Theoretical Physics, University of Tübingen, for warm hospitality and the Alexander von Humboldt Foundation for support.

- [1] M. Ablikim *et al.* (BESIII Collaboration), *Phys. Rev. Lett.* **110**, 252001 (2013).
- [2] Z. Q. Liu *et al.* (Belle Collaboration), *Phys. Rev. Lett.* **110**, 252002 (2013).
- [3] T. Xiao, S. Dobbs, A. Tomaradze, and K. K. Seth, *Phys. Lett. B* **727**, 366 (2013).
- [4] F.-K. Guo, C. Hidalgo-Duque, J. Nieves, and M. P. Valderrama, *Phys. Rev. D* **88**, 054007 (2013); D.-Y. Chen, X. Liu, and T. Matsuki, *Phys. Rev. Lett.* **110**, 232001 (2013); R. Faccini, L. Maiani, F. Piccinini, A. Pilloni, A. D. Polosa, and V. Riquer, *Phys. Rev. D* **87**, 111102 (2013); M. Karliner and S. Nussinov, *J. High Energy Phys.* **07** (2013) 153; N. Mahajan, arXiv:1304.1301; C.-Y. Cui, Y.-L. Liu, W.-B. Chen, and M.-Q. Huang, *Eur. Phys. J. C* **73**, 2661 (2013); Q. Wang, C. Hanhart and Q. Zhao, *Phys. Rev. Lett.* **111**, 132003 (2013); M. B. Voloshin, *Phys. Rev. D* **87**, 091501 (2013); E. Wilbring, H.-W. Hammer, and U.-G. Meißner, *Phys. Lett. B* **726**, 326 (2013); G. Li, *Eur. Phys. J. C* **73**, 2621 (2013); J.-R. Zhang, *Phys. Rev. D* **87**, 116004 (2013); D.-Y. Chen, X. Liu, and T. Matsuki, *ibid.* **88**, 036008 (2013); J. M. Dias, F. S. Navarra, M. Nielsen, and C. M. Zanetti, *ibid.* **88**, 016004 (2013); E. Braaten, arXiv:1305.6905.
- [5] Y. Dong, A. Faessler, T. Gutsche, and V. E. Lyubovitskij, *Phys. Rev. D* **88**, 014030 (2013).
- [6] B. Aubert *et al.* (BaBar Collaboration), *Phys. Rev. Lett.* **95**, 142001 (2005).
- [7] S. R. Blusk, *AIP Conf. Proc.* **870**, 341 (2006).
- [8] K. Abe *et al.* (Belle Collaboration), arXiv:hep-ex/0612006.
- [9] S. -L. Zhu, *Phys. Lett. B* **625**, 212 (2005).
- [10] G.-J. Ding, *Phys. Rev. D* **79**, 014001 (2009).
- [11] Q. Wang, C. Hanhart, and Q. Zhao, *Phys. Rev. Lett.* **111**, 132003 (2013).
- [12] A. Martinez Torres, K. P. Khemchandani, D. Gamermann, and E. Oset, *Phys. Rev. D* **80**, 094012 (2009).
- [13] X. Liu, X.-Q. Zeng, and X.-Q. Li, *Phys. Rev. D* **72**, 054023 (2005).
- [14] C. Z. Yuan, P. Wang, and X. H. Mo, *Phys. Lett. B* **634**, 399 (2006).
- [15] F. J. Llanes-Estrada, *Phys. Rev. D* **72**, 031503 (2005).
- [16] L. Maiani, V. Riquer, F. Piccinini, and A. D. Polosa, *Phys. Rev. D* **72**, 031502 (2005).
- [17] T.-W. Chiu, and T.-H. Hsieh (TWQCD Collaboration), *Phys. Rev. D* **73**, 094510 (2006).
- [18] J. M. Dias, R. M. Albuquerque, M. Nielsen, and C. M. Zanetti, *Phys. Rev. D* **86**, 116012 (2012).
- [19] D.-Y. Chen, J. He, and X. Liu, *Phys. Rev. D* **83**, 054021 (2011).
- [20] E. Kou and O. Pene, *Phys. Lett. B* **631**, 164 (2005).
- [21] F. Iddir and L. Semmla, arXiv:hep-ph/0611183.
- [22] C.-F. Qiao, *Phys. Lett. B* **639**, 263 (2006).
- [23] E. van Beveren and G. Rupp, arXiv:hep-ph/0605317.
- [24] F. Close and C. Downum, *Phys. Rev. D* **79**, 014027 (2009).
- [25] A. Faessler, T. Gutsche, V. E. Lyubovitskij, and Y.-L. Ma, *Phys. Rev. D* **76**, 014005 (2007); **76**, 114008 (2007); **77**, 114013 (2008); A. Faessler, T. Gutsche, S. Kovalenko, and V. E. Lyubovitskij, *ibid.* **76**, 014003 (2007); Y. Dong, A. Faessler, T. Gutsche, and V. E. Lyubovitskij, *ibid.* **77**, 094013 (2008); **79**, 094013 (2009).
- [26] T. Branz, T. Gutsche, and V. E. Lyubovitskij, *Phys. Rev. D* **79**, 014035 (2009).
- [27] T. Branz, T. Gutsche, and V. E. Lyubovitskij, *Phys. Rev. D* **80**, 054019 (2009).
- [28] T. Branz, T. Gutsche, and V. E. Lyubovitskij, *Phys. Rev. D* **82**, 054025 (2010).
- [29] Y. Dong, A. Faessler, T. Gutsche, and V. E. Lyubovitskij, *J. Phys. G* **38**, 015001 (2011).
- [30] Y. Dong, A. Faessler, T. Gutsche, and V. E. Lyubovitskij, *Phys. Rev. D* **81**, 014006 (2010); **81**, 074011 (2010); Y. Dong, A. Faessler, T. Gutsche, S. Kumano, and V. E. Lyubovitskij, *ibid.* **82**, 034035 (2010); **83**, 094005 (2011).
- [31] Y. Dong, A. Faessler, T. Gutsche, and V. E. Lyubovitskij, *J. Phys. G* **40**, 015002 (2013).
- [32] S. Weinberg, *Phys. Rev.* **130**, 776 (1963); A. Salam, *Nuovo Cimento* **25**, 224 (1962); K. Hayashi, M. Hirayama, T. Muta, N. Seto, and T. Shirafuji, *Fortschr. Phys.* **15**, 625 (1967).
- [33] G. V. Efimov and M. A. Ivanov, *The Quark Confinement Model of Hadrons*, (IOP Publishing, Philadelphia, 1993).
- [34] I. V. Anikin, M. A. Ivanov, N. B. Kulimanova, and V. E. Lyubovitskij, *Z. Phys. C* **65**, 681 (1995); M. A. Ivanov, M. P. Locher, and V. E. Lyubovitskij, *Few Body Syst.* **21**, 131 (1996); M. A. Ivanov, V. E. Lyubovitskij, J. G. Körner, and P. Kroll, *Phys. Rev. D* **56**, 348 (1997); S. Dubnicka, A. Z. Dubnickova, M. A. Ivanov, and J. G. Korner, *ibid.* **81**, 114007 (2010); T. Gutsche, M. A. Ivanov, J. G. Korner, V. E. Lyubovitskij, and P. Santorelli, *ibid.* **86**, 074013 (2012); **87**, 074031 (2013).
- [35] T. E. Coan *et al.* (CLEO Collaboration), *Phys. Rev. Lett.* **96**, 162003 (2006).
- [36] X. H. Mo, G. Li, C. Z. Yuan, K. L. He, H. M. Hu, J. H. Hu, P. Wang, and Z. Y. Wang, *Phys. Lett. B* **640**, 182 (2006).
- [37] C. B. Dover, T. Gutsche, and A. Faessler, *Phys. Rev. C* **43**, 379 (1991).
- [38] T. Gutsche, V. E. Lyubovitskij, and M. C. Tichy, *Phys. Rev. D* **79**, 014036 (2009).